REPORT 968

INVESTIGATION AT LOW SPEEDS OF THE EFFECT OF ASPECT RATIO AND SWEEP ON ROLLING STABILITY DERIVATIVES OF UNTAPERED WINGS

By Alex Goodman and Lewis R. Fisher

SUMMARY

A low-scale wind-tunnel investigation was conducted in rolling flow to determine the effects of aspect ratio and sweep (when varied independently) on the rolling stability derivatives for a series of untapered wings. The rolling-flow equipment of the Langley stability tunnel was used for the tests.

The results of the tests indicate that, when the aspect ratio is held constant, an increase in the sweepback angle causes a significant reduction in the damping in roll at low lift coefficients for only the higher aspect ratios tested. This result is in agreement with available swept-wing theory which indicates no effect of sweep for aspect ratios near zero. The result of the linear theory that the damping in roll is independent of lift coefficient and that the yawing moment and lateral force due to rolling are directly proportional to the lift coefficient was found to be valid for only a very limited lift-coefficient range when the wings were highly swept. For such wings, the damping was found to increase in magnitude and the yawing moment due to rolling, to change from negative to positive at moderate lift coefficients.

The effect of wing-tip suction, not accounted for by present theory, was found to be very important with regard to the yawing moment due to rolling, particularly for low-aspect-ratio swept wings. An empirical means of correcting present theory for the effect of tip suction is suggested.

The data of the present investigation have been used to develop a method of accounting for the effects of the drag on the yawing moment due to rolling throughout the lift range.

INTRODUCTION

In order to estimate the dynamic flight characteristics of an airplane, a knowledge of the stability derivatives is necessary. The static-stability derivatives are easily determined from conventional wind-tunnel tests. The rotary derivatives, however, have usually been estimated in the past from available theory because of the lack of a convenient experimental technique. Such a technique has been developed, and the rotary derivatives can now be easily determined by the utilization of the curved-flow and rolling-flow equipment in the Langley stability tunnel. This equipment is being utilized for the purpose of determining the effects of various geometric variables on the rotary and static stability characteristics of wings and complete airplane configurations. The method of determining the rolling derivatives by means of the rolling-flow equipment is described in reference 1.

The present report gives results of tests made to determine the effects of independent variations of aspect ratio and sweep on the rolling derivatives of a series of untapered wings. The static and yawing derivatives determined for the same wings are reported in reference 2. Data obtained in the present investigation have been used to derive an empirical correction to existing theory for evaluation of the derivative of yawing moment due to rolling.

SYMBOLS

The data are presented in the form of standard NACA coefficients of forces and moments, which are referred in all cases to the stability axes with the origin at the quarter-chord point of the mean aerodynamic chord of the models tested. The positive directions of the forces, moments, and angular displacements are shown in figure 1. The coefficients and symbols used herein are defined as follows:

C_L	lift coefficient (L/qS)
C_D	drag coefficient $(-X/qS)$
C_Y	lateral-force coefficient (Y/qS)
C_l	rolling-moment coefficient (L'/qSb)
C_n	yawing-moment coefficient (N/qSb)
L	lift
X	longitudinal force
Y	lateral force
Z	normal force
L'	rolling moment
M	pitching moment
N	yawing moment
q	dynamic pressure $(\frac{1}{2}\rho V^2)$
ρ	mass density of air
V	free-stream velocity
S	wing area
b	span of wing, measured perpendicular to plane of symmetry
c	chord of wing, measured parallel to plane of symmetry
$\bar{c}$	mean aerodynamic chord $\left(\frac{2}{S}\int_0^{b/2} c^2\,dy\right)$
y	distance measured perpendicular to plane of symmetry
x	distance of quarter-chord point of any chordwise section from leading edge of root chord measured parallel to plane of symmetry

$\bar{x}$ distance from leading edge of root chord to wing aerodynamic center $\left(\frac{2}{S}\int_0^{b/2} cx\,dy\right)$

d longitudinal distance from midchord point at wing tip to coordinate origin

x' longitudinal distance rearward from coordinate origin (center of gravity) to wing aerodynamic center

A aspect ratio (b^2/S)

λ taper ratio (Tip chord/Root chord)

α angle of attack, measured in plane of symmetry

Λ angle of sweep, degrees

$pb/2V$ wing-tip helix angle, radians

p rolling angular velocity, radians per second

$C_{L_\alpha}=\frac{\partial C_L}{\partial \alpha}$

$C_{D_\alpha}=\frac{\partial C_D}{\partial \alpha}$

$C_{Y_p}=\frac{\partial C_Y}{\partial\left(\frac{pb}{2V}\right)}$

$C_{n_p}=\frac{\partial C_n}{\partial\left(\frac{pb}{2V}\right)}$

$C_{l_p}=\frac{\partial C_l}{\partial\left(\frac{pb}{2V}\right)}$

APPARATUS AND TESTS

The tests of the present investigation were conducted in the 6-foot-diameter rolling-flow test section of the Langley stability tunnel. In this test section, rolling flight is simulated by rotating the air stream about a rigidly mounted model. (See reference 1.)

The models tested consisted of a series of untapered wings, all of which had NACA 0012 airfoil sections in planes normal to the leading edge. The model configurations are identified by the following designations:

Wing	Aspect ratio	Sweepback (deg)
1	1.34	0
2	1.34	45
3	1.34	60
4	2.61	0
5	2.61	45
6	2.61	60
7	5.16	0
8	5.16	45
9	5.16	60

The wing plan forms and other pertinent model data are presented in figure 2.

The models were rigidly mounted on a single strut at the quarter-chord point of the mean aerodynamic chord. (See fig. 3.) The forces and moments were measured by means of electrical strain gages mounted on the strut.

All of the tests were made at a dynamic pressure of 39.7 pounds per square foot (Mach number of 0.17) with the exception of the tests made on wing 9. The tests on this wing were made at a dynamic pressure of 24.9 pounds per square foot (Mach number of 0.13) because of the flexibility of the model. The Reynolds numbers for these tests are presented in table I. In the present investigation, tests were made through a range of rotor speeds corresponding to the values of $pb/2V$ given in table I. Each model was tested through an angle-of-attack range from approximately zero lift up to and beyond maximum lift.

As part of this investigation, the effects of sharp-nose airfoil sections on the rotary derivatives were also determined. The sharp-nose airfoil sections were simulated by attaching full-span leading-edge spoilers to wings 1 and 4 (fig. 2).

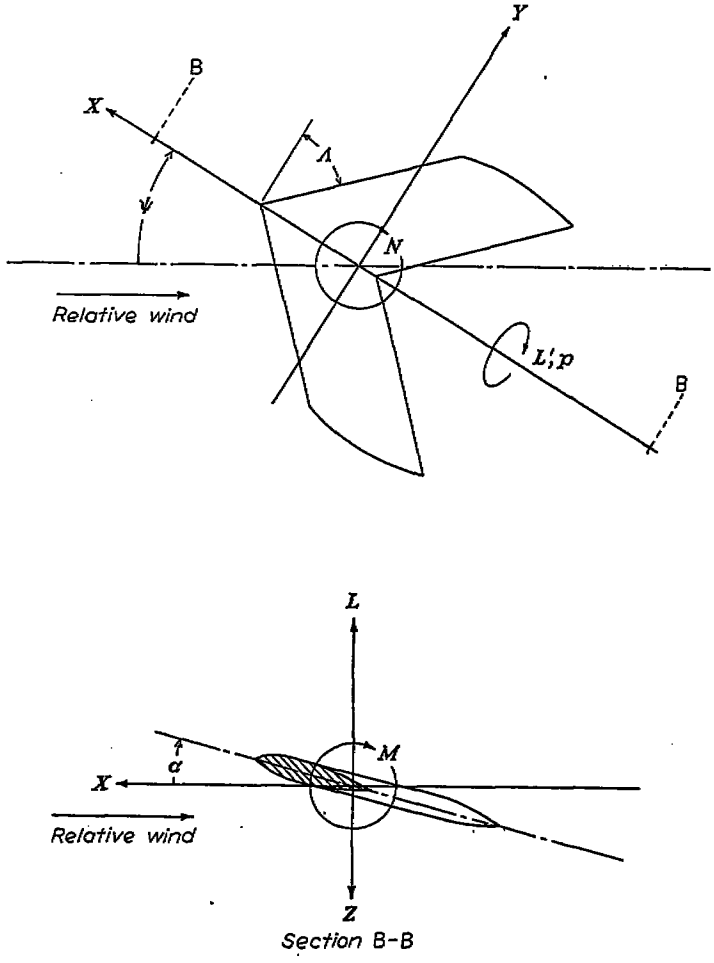

FIGURE 1.—System of axes used. Positive directions of forces, moments, and angles are indicated.

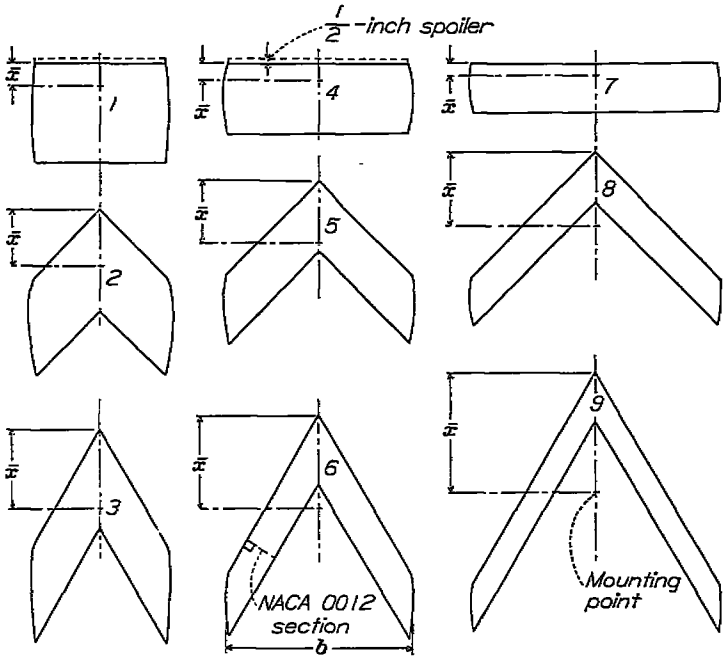

Λ (deg)	Wing	A	S (sq ft)	b (ft)	c̄ (ft)	x̄ (ft)
0	1	1.34	3.64	2.21	1.68	0.41
	4	2.61	3.60	3.08	1.18	.30
	7	5.16	3.52	4.26	.83	.21
45	2	1.34	3.62	2.20	1.66	0.96
	5	2.61	3.56	3.05	1.17	1.05
	8	5.16	3.50	4.26	.83	1.26
60	3	1.34	3.64	2.21	1.65	1.36
	6	2.61	3.53	3.05	1.16	1.60
	9	5.16	3.56	4.28	.83	2.06

FIGURE 2.—Plan forms of sweptback wings. NACA 0012 profile (perpendicular to leading edge)

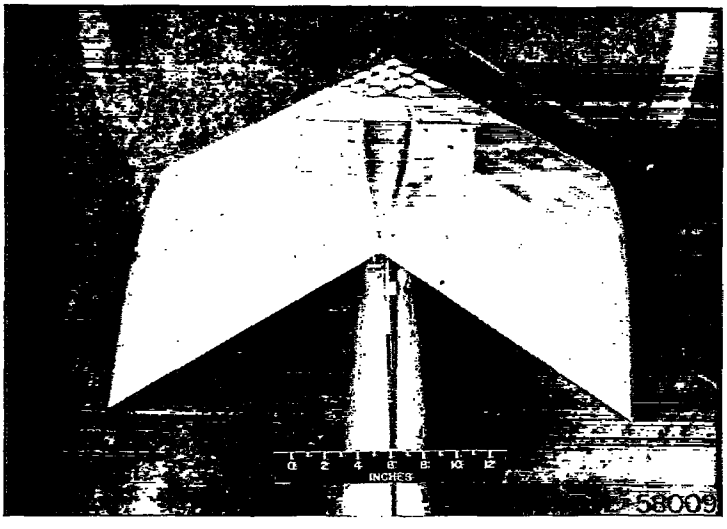

(a) Wing 2. $A=1.34$; $\Lambda=45°$.

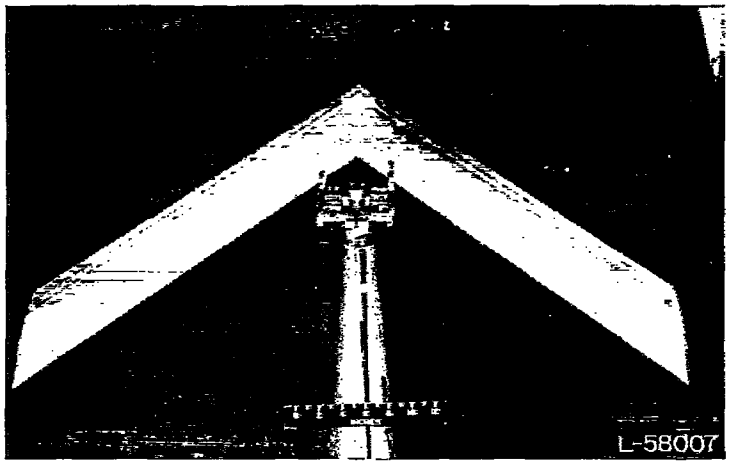

(b) Wing 8. $A=5.16$; $\Lambda=45°$.

FIGURE 3.—Wings mounted in the 6-foot-diameter rolling-flow test section of the Langley stability tunnel.

TABLE I.—TEST CONDITIONS AND CONFIGURATIONS

Sweep angle, Λ (deg)	Aspect ratio, A	Reynolds number based on c and V	Wing-tip helix angle, $\frac{pb}{2V}$
0	1.34	1.99×10^6	0, ±0.0149, ±0.0448
0	2.61	1.39	0, ±.0208, ±.0625
0	5.16	.98	0, ±.0288, ±.0664
45	1.34	1.97	0, ±.0149, ±.0446
45	2.61	1.39	0, ±.0212, ±.0619
45	5.16	.97	0, ±.0288, ±.0664
60	1.34	1.97	0, ±.0149, ±.0448
60	2.61	1.37	0, ±.0212, ±.0619
60	5.16	.76	0, ±.0355, ±.1064

CORRECTIONS

Corrections for the effects of jet boundaries, based on unswept-wing theory, have been applied to the angle of attack, drag coefficient, and rolling-moment-coefficient data.

No corrections for the effects of blocking, turbulence, or for the effects of static-pressure gradient on the boundary-layer flow have been applied.

RESULTS AND DISCUSSION

PRESENTATION OF DATA

The results of the present series of tests are presented in figures 4 to 17. The lift coefficient and drag coefficient not ideally associated with lift $C_D-\frac{C_L^2}{\pi A}$ for the present series of wings are presented in figure 4 and were obtained from tests of reference 2. The rolling stability characteristics for the wings with and without spoilers are given in figures 5 to 8. The development of the method used to calculate the yawing moment due to rolling throughout the lift range is presented in figures 9 to 15. A comparison between the experimental and calculated values of the yawing moment due to rolling is given in figures 16 and 17.

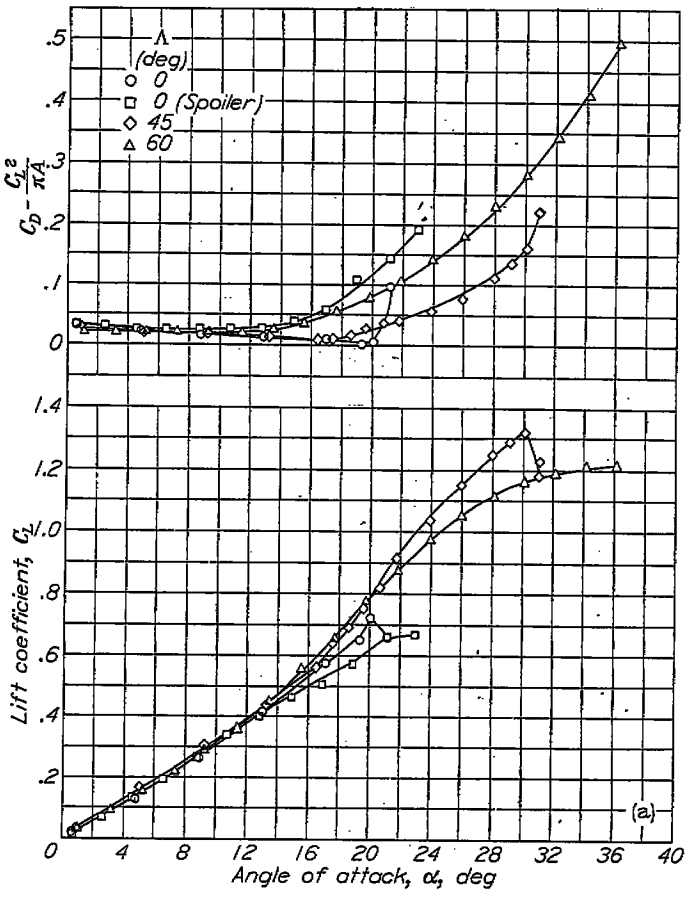

(a) A=1.34.

FIGURE 4.—Variation with angle of attack of the aerodynamic characteristics of a series of swept wings.

DAMPING IN ROLL

Results obtained for the damping in roll (fig. 5) show that for the low-aspect-ratio wings (A=1.34 and 2.61) variations in the sweep angles produced rather irregular effects. At the lowest aspect ratio, the damping in roll of the wings with 45° and 60° sweepback was greater than that of the unswept wing, and the difference was greater at high lift coefficients than at low lift coefficients. For an aspect ratio of 2.61, the damping in roll increased abruptly at lift coefficients of about 0.3 and 0.6 for the 60° and 45° sweptback wings, respectively; whereas, no abrupt change was noted for the unswept wing except at maximum lift. The abrupt changes in damping in roll occur at approximately the lift coefficients at which the drag increment $C_D-\frac{C_L^2}{\pi A}$ begins to increase. (See fig. 4 (b).) Changes in the damping in roll (as well as in other rotary and static derivatives) might be expected because an increase in the increment $C_D-\frac{C_L^2}{\pi A}$ should correspond to the beginning of

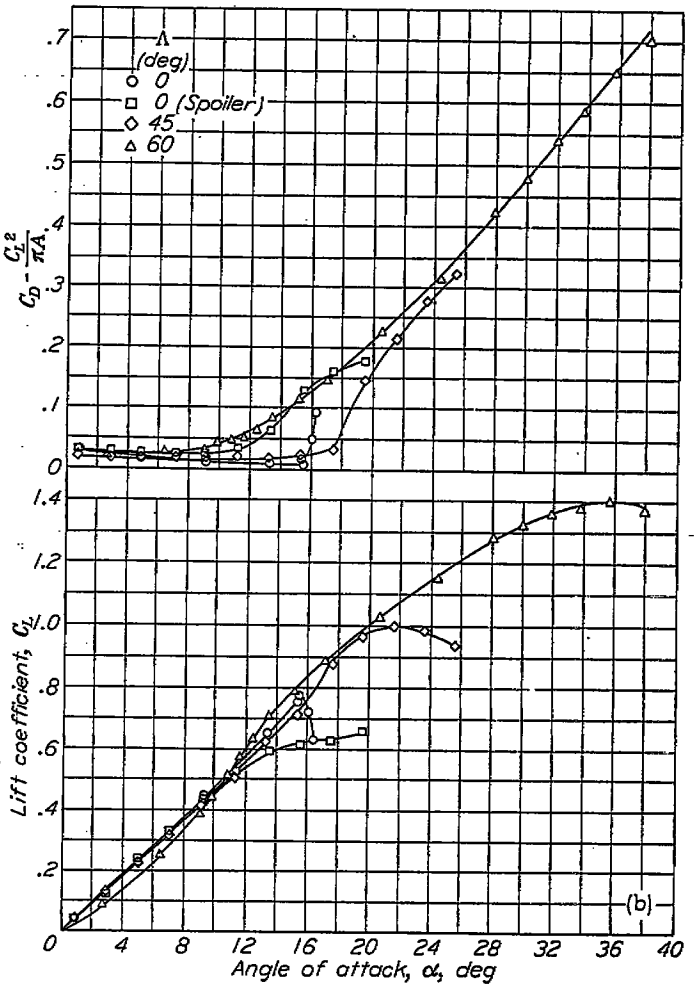

(b) A=2.61.

FIGURE 4.—Continued.

flow separation from some point on the wing surface. Appreciably sharper breaks in the curves of $C_D - \frac{C_L^2}{\pi A}$ were obtained for the sweptback wings having an aspect ratio of 5.16. (See fig. 4 (c).) The breaks occur at lift coefficients of about 0.3 and 0.5 for the wings with 60° and 45° sweepback, respectively, which are in fair agreement with the lift coefficients at which breaks occur in the damping-in-roll curves (fig. 5).

An increase in Reynolds number, which would delay separation and consequently cause the increases in $C_D - \frac{C_L^2}{\pi A}$ to occur at higher lift coefficients, probably would also extend the linear portions of the curves of damping in roll and of the other rotary derivatives.

The experimental values of C_{l_p} for $C_L=0$ determined from these tests are compared with the theoretical values obtained from the approximate theory of reference 3 and by an application of the theory of Weissinger as presented in reference 4. (See fig. 6.) The variation of C_{l_p} for $C_L=0$ as given by reference 3 is

$$C_{l_p} = \frac{(A+4)\cos\Lambda}{A+4\cos\Lambda}(C_{l_p})_{\Lambda=0}$$

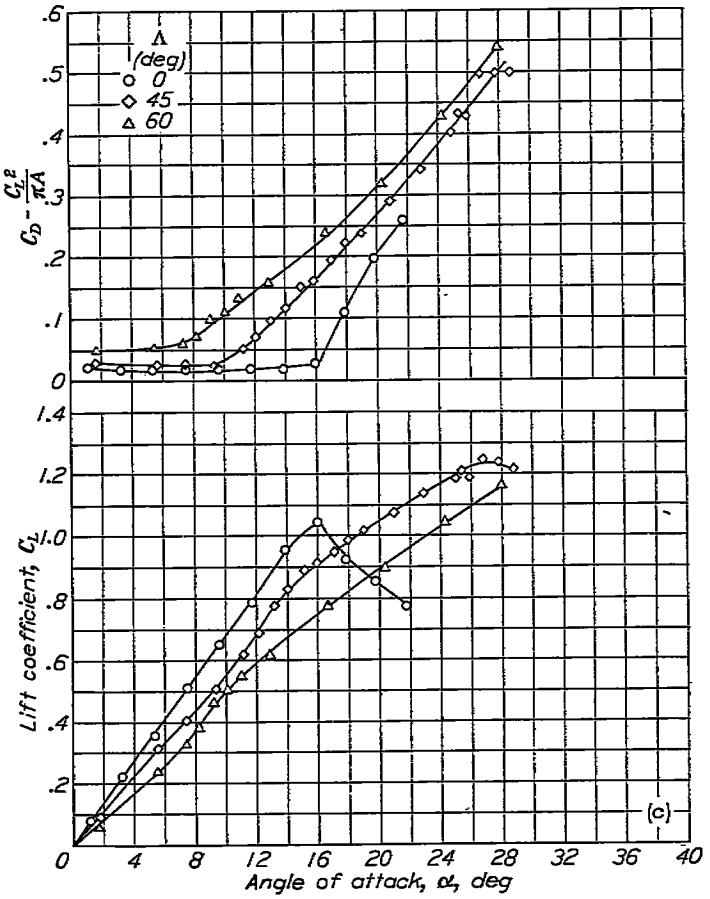

(c) $A=5.16$.

FIGURE 4.—Concluded.

where $(C_{l_p})_{\Lambda=0}$ for $C_L=0$ is obtained from the best available theory or experimental data. A section-lift-curve slope of 5.67 per radian was used for both the Weissinger and approximate theory computations. In general, the experimental data compare about equally well with either of the theories. Both theories indicate a decreased effect of sweep as the aspect ratio is reduced, although the variations indicated by reference 4 appear to be somewhat more reliable than those indicated by reference 3, particularly at low aspect ratios.

Full-span leading-edge spoilers tested on two unswept wings (wings 1 and 4) had little effect on C_{l_p} over a greater part of the lift range. (See fig. 7.) At high lift coefficients, a definite reversal in the sign of C_{l_p} was obtained slightly before maximum lift was reached. A reversal in the sign of C_{l_p} for the wings without spoilers could not be established because near maximum lift the model vibrated so severely that accurate measurements could not be made.

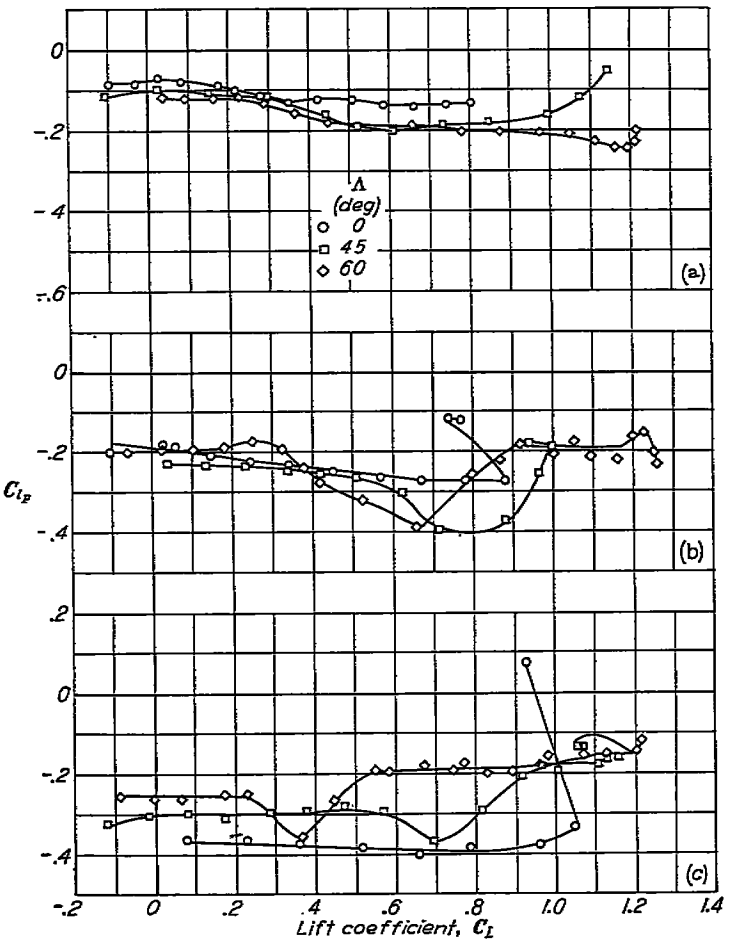

(a) $A=1.34$.
(b) $A=2.61$.
(c) $A=5.16$.

FIGURE 5.—Variation of C_{l_p} with lift coefficient.

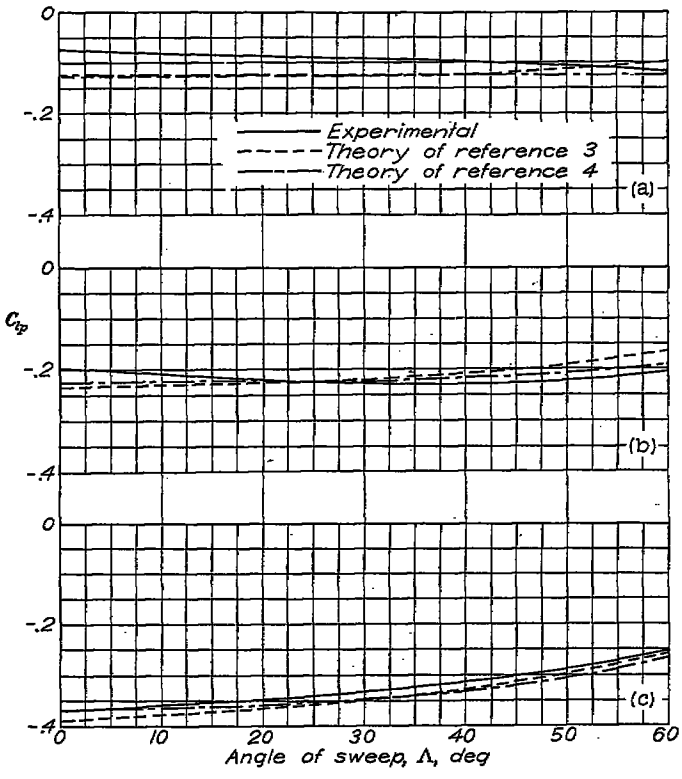

(a) $A=1.34$.
(b) $A=2.61$.
(c) $A=5.16$.

FIGURE 6.—Variation of C_{l_p} for zero lift with sweep angle.

LATERAL FORCE DUE TO ROLLING

The derivative C_{Y_p} varies linearly with lift coefficient in most cases for only a limited range of lift coefficients. (See fig. 8.) The slopes C_{Y_p}/C_L through zero lift are compared in figure 10 with values obtained by the approximate theory of reference 3. Both theory and experiment indicate an increase in slope with sweep for constant aspect ratio. The agreement between theory and experiment is poor, however, at the lower aspect ratios. The theory of reference 3 does not account for the values of C_{Y_p}/C_L obtained at zero sweep. These values are presumed to be caused by tip suction (analogous to leading-edge suction discussed in reference 5). For the wings considered, the effect of tip suction appears to be approximately independent of the sweep angle, because the differences between the experimental and theoretical curves are almost the same at all sweep angles, although the magnitude of the difference increases appreciably as the aspect ratio is reduced. The theory of low-aspect-ratio triangles presented in reference 5 indicates that the contribution of tip suction to the derivative C_{Y_p} varies inversely as the aspect ratio. If the same relationship is assumed to apply to the present wings, an empirical expression for the effect of tip suction can be determined by plotting C_{Y_p}/C_L for zero sweep against $1/A$. Such a plot, obtained from the present data and from unpublished data on a tapered wing, is presented in figure 9. The data fall consistently below the curve indicated by reference 5 for low-aspect-ratio triangles but are in fair agreement with the following empirical expression:

$$\left(\frac{C_{Y_p}}{C_L}\right)_{\Lambda=0}=\frac{1}{A} \tag{1}$$

When this increment is added to the contribution caused by sweep, as given in reference 3, the following equation results:

$$\frac{C_{Y_p}}{C_L}=\frac{A+\cos\Lambda}{A+4\cos\Lambda}\tan\Lambda+\frac{1}{A} \tag{2}$$

Results calculated from equation (2) are compared in figure 10 with the experimental results. The fact that good agreement is obtained is of little interest, since the same experimental results were used to evaluate the empirical correction included in equation (2). The most important application of the tip-suction increment of C_{Y_p} is in connection with the derivative C_{n_p} as discussed in the section entitled "Yawing Moment Due to Rolling."

YAWING MOMENT DUE TO ROLLING

For the unswept wings without spoilers, wings 4 and 7, the variation of C_{n_p} with lift coefficient was approximately linear up to maximum lift coefficient. The variation of C_{n_p} with lift coefficient for wing 1 (without spoiler) was linear for only the low-lift-coefficient range. (See fig. 11.) The sharp leading-edge wings, as simulated by attaching full-span leading-edge spoilers to wings 1 and 4, yielded about the same values of C_{n_p} at low lift coefficients as when no spoilers were attached. (See fig. 7.) At moderate lift coefficients, the spoilers caused a reversal in the sign of C_{n_p}, and C_{n_p} became positive. This variation is similar to the variation obtained with the swept wings. (See figs. 7 and 11.)

The values of C_{n_p} for the swept wings were proportional to the lift coefficient for only a limited range. At moderate lift coefficients, C_{n_p} reversed sign and assumed comparatively large positive values. This change probably results from the high drag associated with partial separation. Also, the initial slope C_{n_p}/C_L (fig. 13) increases as the aspect ratio decreases. The theory of references 3 and 6 indicates the opposite variation. A possible explanation for the observed trend might be that the tip-suction contribution to the lateral force also contributes to the yawing moment. If the resultant tip-suction force is assumed to act at the midchord point of the wing tip, a correction to C_{n_p} can easily be derived from the empirical expression previously obtained for the tip-suction force. The correction is

$$\frac{\Delta C_{n_p}}{C_L}=-\left(\frac{C_{Y_p}}{C_L}\right)_{\Lambda=0}\frac{d}{b}$$

where C_{Y_p}/C_L for $\Lambda=0°$ is given by equation (1) and d, the longitudinal distance from the midchord point at the wing tip to the coordinate origin, is

$$d=\frac{b}{4}\tan\Lambda+\frac{b}{4A}+x'$$

where x' is the longitudinal distance rearward from the coordinate origin (center of gravity) to the wing aerodynamic center. Therefore, for untapered wings

$$\frac{\Delta C_{n_p}}{C_L}=-\frac{1}{4A}\left(\tan\Lambda+\frac{1}{A}\right)-\frac{1}{A^2}\frac{x'}{\bar{c}} \tag{3}$$

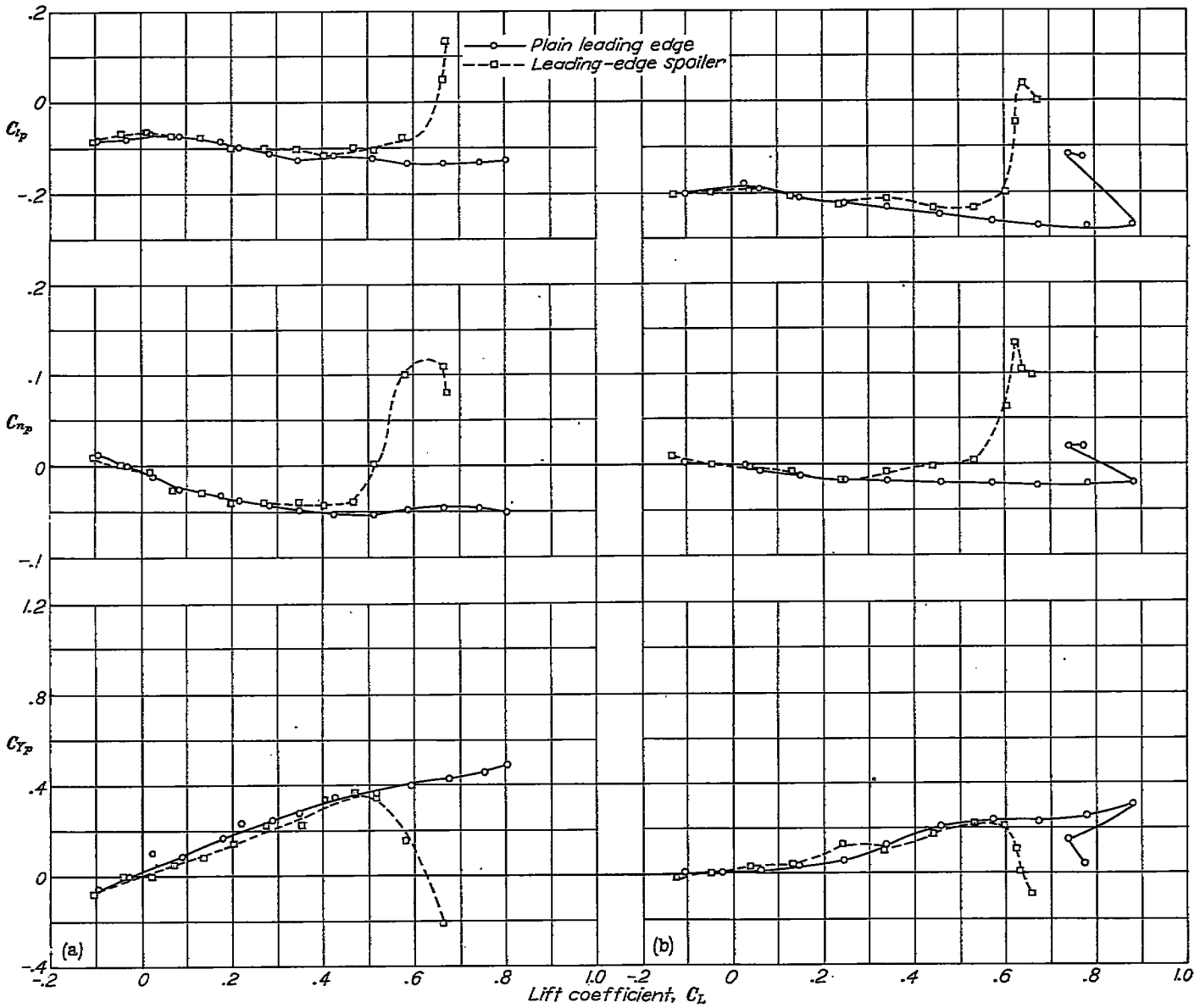

(a) $\Lambda=0°$; $A=1.34$. (b) $\Lambda=0°$; $A=2.61$.

FIGURE 7.—Effect of leading-edge spoiler on the rolling derivatives of two unswept wings.

which when added to equation (31) of reference 3 gives

$$\frac{(\Delta C_{n_p})_1}{C_L}=\frac{A+4}{A+4\cos\Lambda}\left[1+6\left(1+\frac{\cos\Lambda}{A}\right)\left(\frac{x'}{\bar{c}}\frac{\tan\Lambda}{A}+\frac{\tan^2\Lambda}{12}\right)\right]\left(\frac{C_{n_p}}{C_L}\right)_0-\frac{1}{4A}\left(\tan\Lambda+\frac{1}{A}\right)-\frac{1}{A^2}\frac{x'}{\bar{c}} \quad (4)$$

The quantity $(C_{n_p}/C_L)_0$ was given as $(C_{n_p}/C_L)_{\Lambda=0}$ in reference 3, but the new symbol is used herein since this quantity does not include tip suction. (Equation (3) does not reduce to zero at $\Lambda=0°$.)

Equation (4) has been used to construct the chart shown in figure 12. The symbol $\frac{(\Delta C_{n_p})_1}{C_L}$ indicates that the chart applies only to that part of C_{n_p} contributed by the lift and induced-drag forces. Figure 13 shows a comparison of the experimental and calculated values of C_{n_p}/C_L. The revised equation results in appreciable improvement over the equation of reference 3. The agreement is very good for all the wings tested.

As indicated by figure 11 the curves of C_{n_p} against C_L are linear over only a small range for the swept wings because of the rise in drag at high lift coefficients. An equation which includes consideration of the effect of the drag for unswept wings is given in reference 7 as

$$C_{n_p}=-K(C_L-C_{D_\alpha}) \quad (5)$$

where the value of K depends on the plan form of the wing. If the induced drag is separated from the profile drag, equation (5) can be written as

$$C_{n_p}=-KC_L\left(1-2\frac{C_{L_\alpha}}{\pi A}\right)+K(C_{D_0})_\alpha \quad (6)$$

where

$$(C_{D_0})_\alpha=\frac{\partial}{\partial\alpha}\left(C_D-\frac{C_L^2}{\pi A}\right)$$

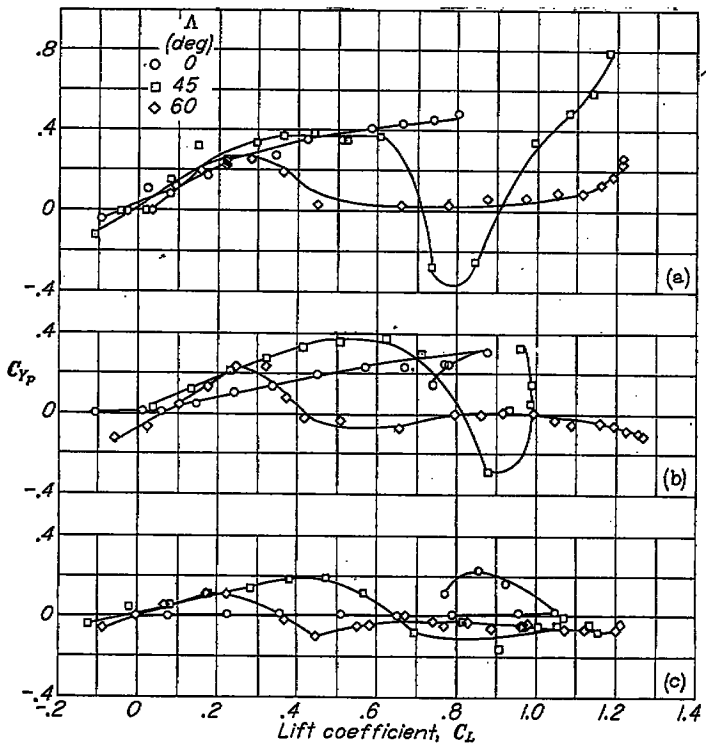

(a) A=1.34.
(b) A=2.61.
(c) A=5.16.

FIGURE 8.—Variation of C_{Y_p} with lift coefficient.

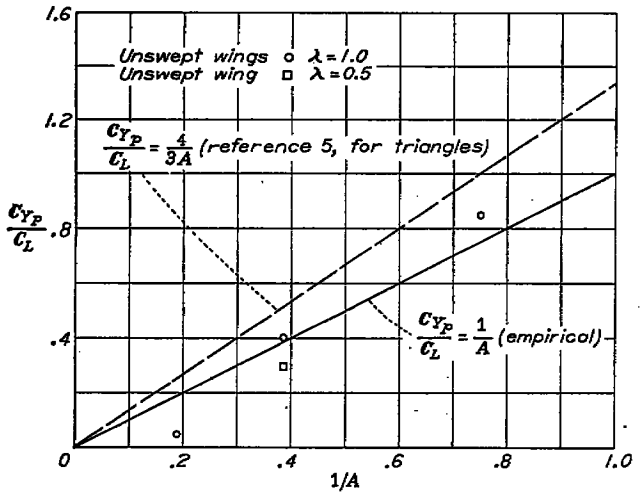

FIGURE 9.—Variation of C_{Y_p}/C_L with $1/A$ for several unswept wings.

For swept wings, the first term of equation (6) can presumably be replaced by equation (4) and, therefore,

$$C_{n_p}=\frac{(\Delta C_{n_p})_1}{C_L}C_L+K(C_{D_0})_\alpha \tag{7}$$

The increment of C_{n_p} not associated with the lift or induced-drag forces, therefore, can be expressed as

$$(\Delta C_{n_p})_2=K(C_{D_0})_\alpha \tag{8}$$

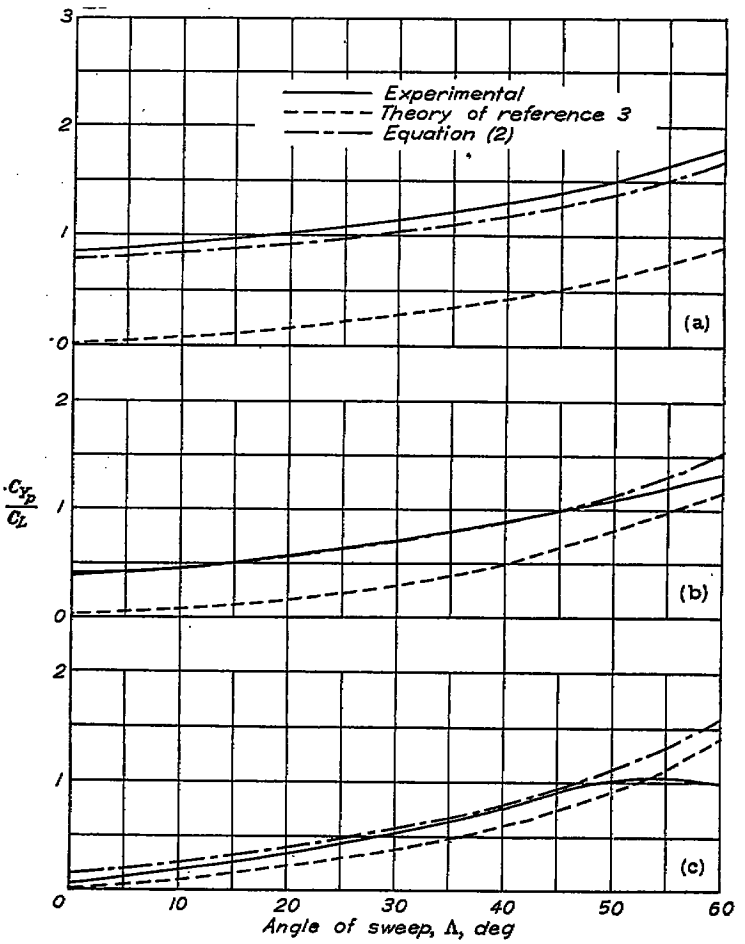

(a) A=1.34.
(b) A=2.61.
(c) A=5.16.

FIGURE 10.—Variation of C_{Y_p}/C_L with sweep angle.

The value of the constant K can be evaluated empirically, since $(C_{D_0})_\alpha$ can be obtained by measuring the slopes of the curves of $C_D-\frac{C_L^2}{\pi A}$ plotted against angle of attack in figure 4, and

$$(\Delta C_{n_p})_2=C_{n_p}-(\Delta C_{n_p})_1$$

where C_{n_p} is the experimental value and $(\Delta C_{n_p})_1$ is obtained from figure 12. In evaluating $(C_{D_0})_\alpha$ any initial slope at zero lift was subtracted from the slope at a specific angle of attack because, for the symmetrical wings considered, the initial slope must have resulted from support-strut interference.

Values of $(\Delta C_{n_p})_2$ are plotted against $(C_{D_0})_\alpha$ in figure 14.

The slopes of the curves appear to depend on aspect ratio, but no consistent variation with sweep angle exists. The average slopes of the data of figure 14 are plotted against aspect ratio in figure 15. At high aspect ratios the value of the constant K approaches that given by Zimmerman (reference 7), but at low aspect ratios the empirical values are much higher.

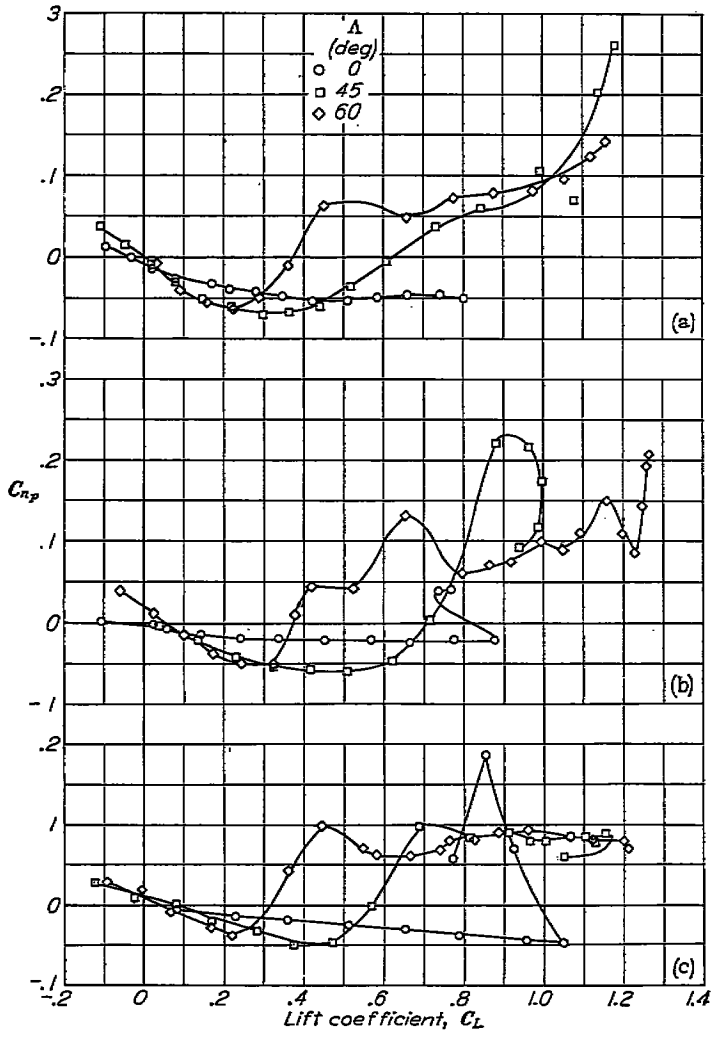

(a) $A=1.34$.
(b) $A=2.61$.
(c) $A=5.16$.

FIGURE 11.—Variation of C_{n_p} with lift coefficient.

Equation (7) was used to calculate C_{n_p} throughout the lift range for the wings of the present investigation and for several others (unpublished). The experimental and calculated values of C_{n_p} for these cases are presented in figures 16 and 17.

The wings considered in figure 16 are the wings of the present investigation which was used to develop the empirical corrections to the theory and, therefore, the fact that reasonably good agreement between calculations and experiment was obtained might not be considered as a valid verification of the method. The wings considered in figure 17, however, include the unswept wings wth leading-edge spoilers of the present investigation and certain additional wings from other unpublished investigations. In general, the agreement shown in figure 17 is approximately as good as that shown in figure 16. Two of the wings in figure 17 were tapered (taper ratios of 0.50 and 0.25). The agreement obtained with these tapered wings is approximately as good as that obtained for untapered wings, in spite of the fact that the method was developed for untapered wings.

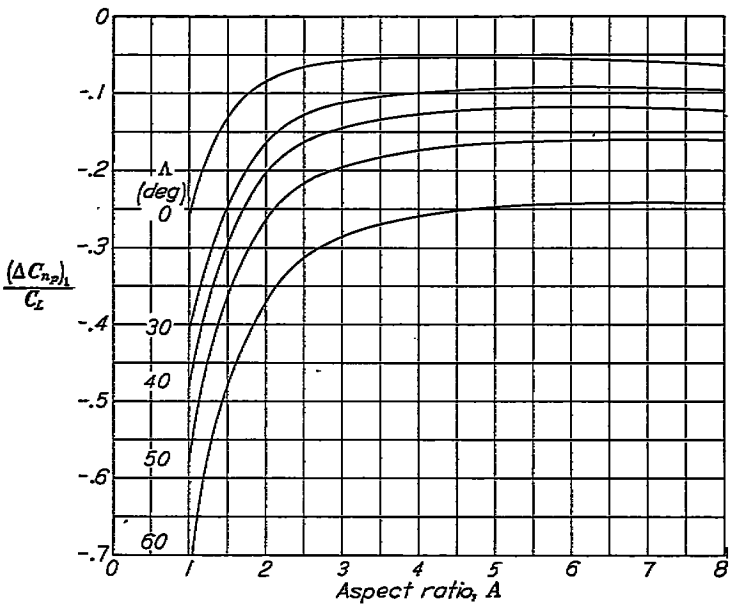

FIGURE 12.—Variation of the increment of C_{n_p} (due to the lift and induced drag forces) with aspect ratio. Equation (4).

CONCLUSIONS

The results of low-scale wind-tunnel tests made in rolling flow to determine the effects of aspect ratio and sweep (when varied independently) on the rolling stability derivatives for a series of untapered wings indicated the following conclusions:

1. When the aspect ratio is held constant, an increase in the sweepback angle causes a significant reduction in the damping in roll at low lift coefficients for only the higher aspect ratios tested. The result is in agreement with available swept-wing theory which indicates no effect of sweep for aspect ratios near zero.

2. The result of linear theory that the damping in roll is independent of the lift coefficient and that the yawing moment and lateral force due to rolling are directly proportional to the lift coefficient was found to be valid for only a very limited lift-coefficient range when the wings were highly swept. For such wings, the damping in roll was found to increase in magnitude and the yawing moment due to rolling, to change from negative to positive at moderate lift coefficients.

3. The effect of wing-tip suction, not accounted for by present theory, was found to be very important with regard to the yawing moment due to rolling, particularly for low-aspect-ratio swept wings. An empirical means of correcting the present theory for the effect of tip suction is suggested.

4. The data of the present investigation have been used to develop a method of accounting for the effects of the drag on the yawing moment due to rolling throughout the lift range.

LANGLEY AERONAUTICAL LABORATORY,
NATIONAL ADVISORY COMMITTEE FOR AERONAUTICS,
LANGLEY AIR FORCE BASE, VA., *January 19, 1949.*

950646—51——25

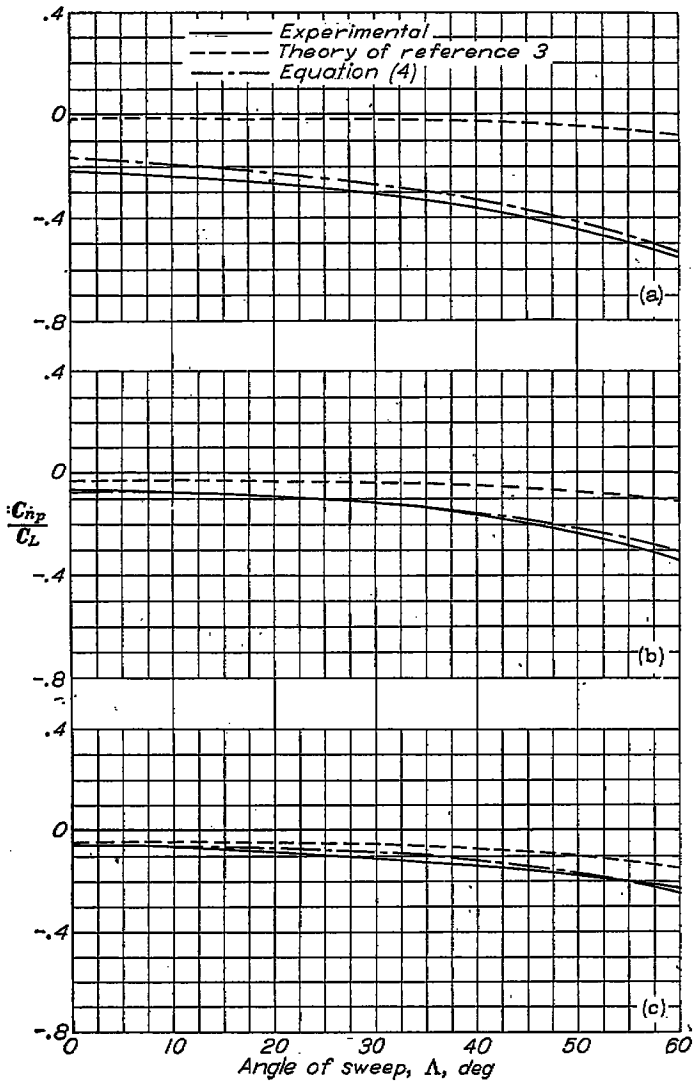

(a) A=1.34.
(b) A=2.61.
(c) A=5.16.

FIGURE 13.—Variation of C_{n_p}/C_L with sweep angle.

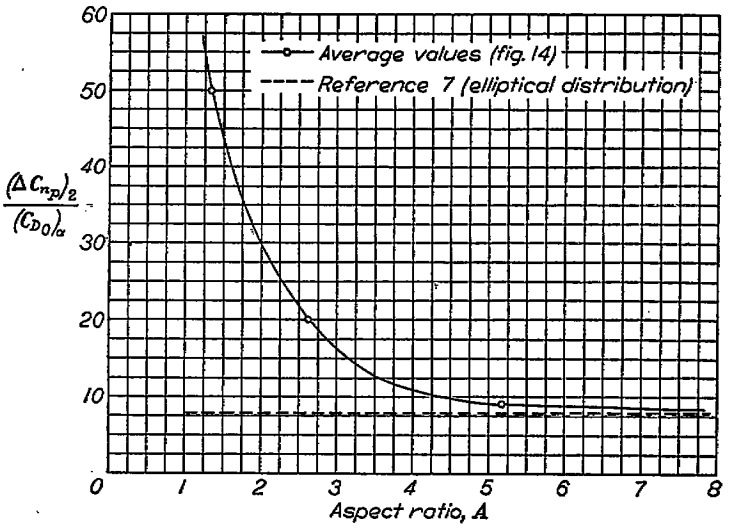

FIGURE 15.—Variation of $\frac{(\Delta C_{n_p})_2}{(C_{D_0})_\alpha}$ with aspect ratio.

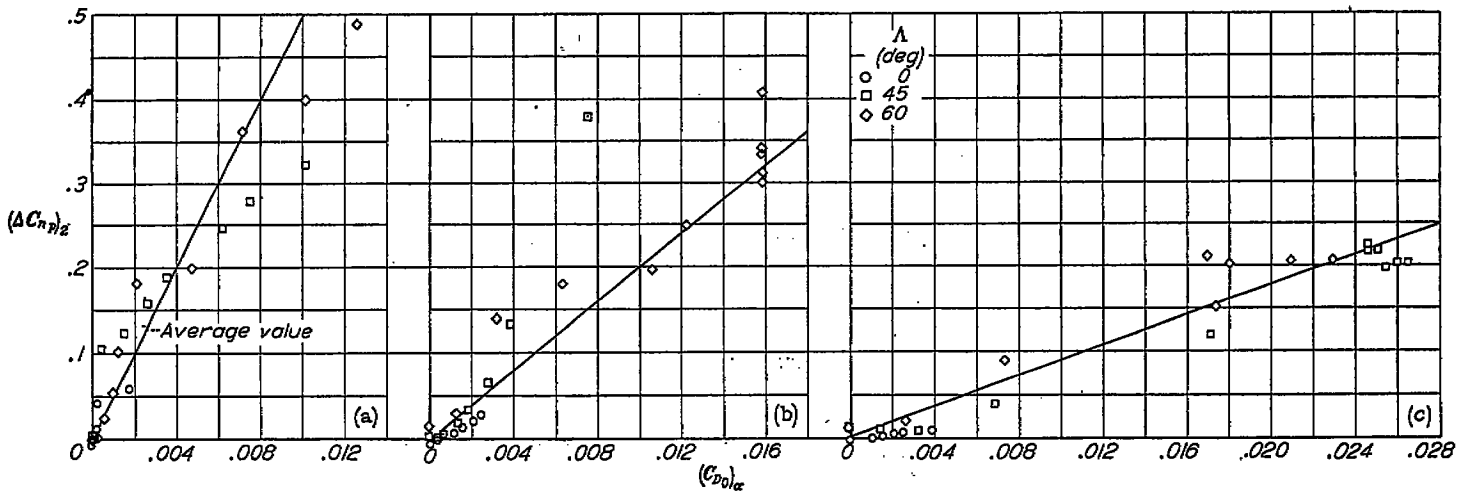

(a) A=1.34. (b) A=2.61. (c) A=5.16.

FIGURE 14.—Variation of the increment of C_{n_p} (increment not associated with lift or induced drag forces) with $(C_{D_0})_\alpha$. Equation (8).

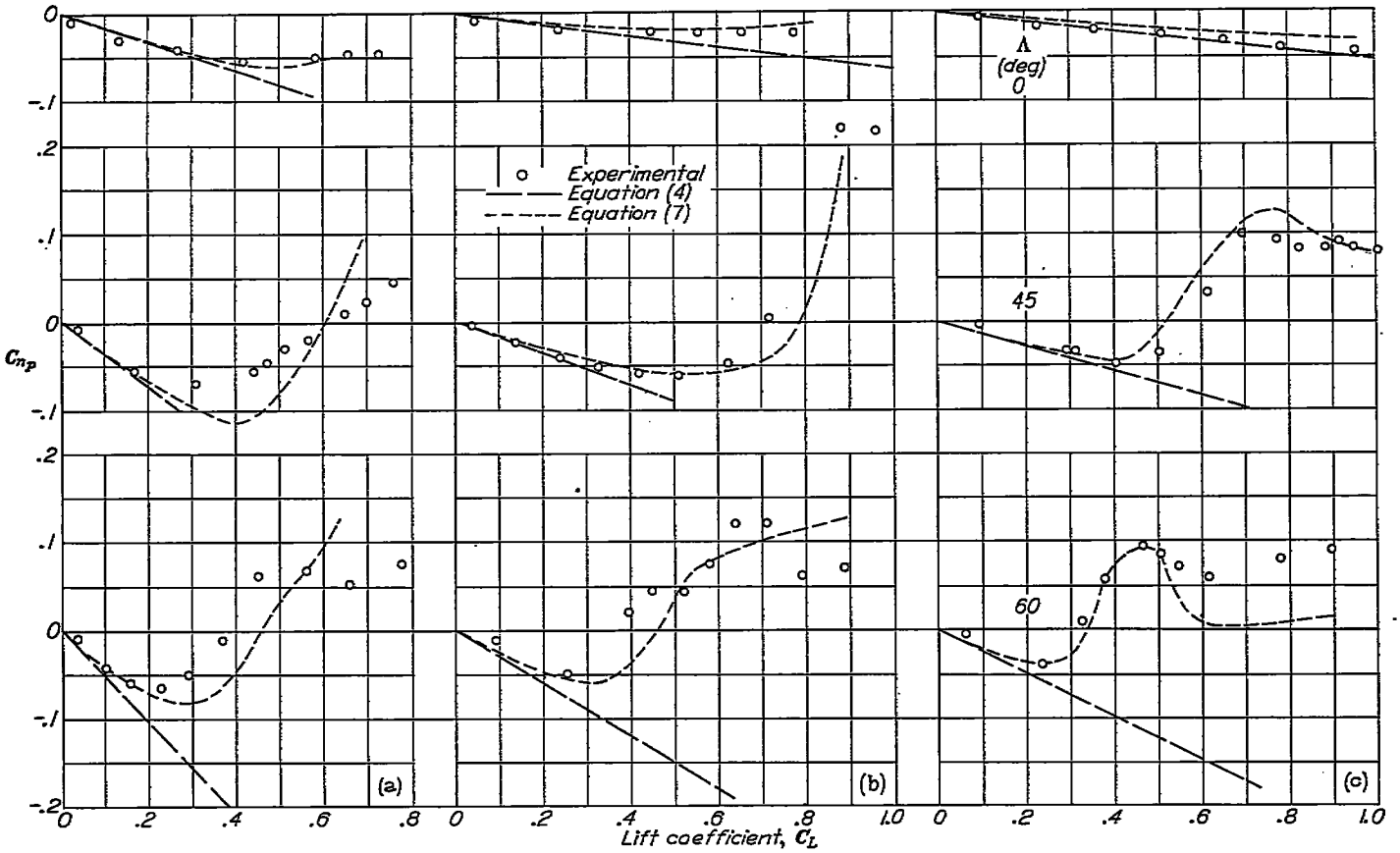

(a) A=1.34. (b) A=2.61. (c) A=5.16.

FIGURE 16.—Variation of the experimental and calculated values of C_{n_p} with lift coefficient for a series of swept wings.

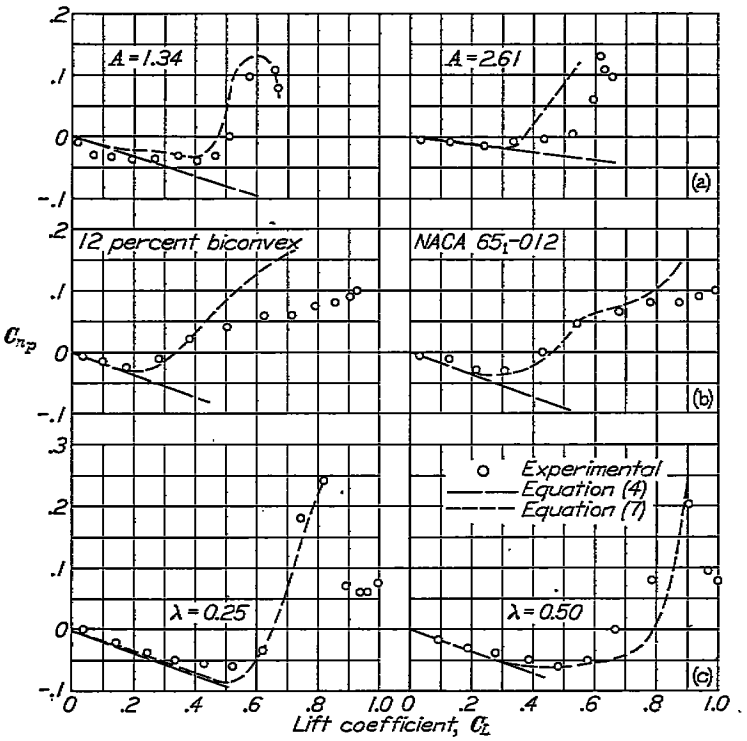

(a) Λ=0; nose spoilers.
(b) A=2.61; Λ=45°.
(c) A=2.61; Λ=45°.

FIGURE 17.—Comparison of additional experimental and calculated values of C_{n_p} for several swept wings.

REFERENCES

1. MacLachlan, Robert, and Letko, William: Correlation of Two Experimental Methods of Determining the Rolling Characteristics of Unswept Wings. NACA TN 1309, 1947.
2. Goodman, Alex, and Brewer, Jack D.: Investigation at Low Speeds of the Effect of Aspect Ratio and Sweep on Static and Yawing Stability Derivatives of Untapered Wings. NACA TN 1669, 1948.
3. Toll, Thomas A., and Queijo, M. J.: Approximate Relations and Charts for Low-Speed Stability Derivatives of Swept Wings. NACA TN 1581, 1948.
4. Bird, John D.: Some Theoretical Low-Speed Span Loading Characteristics of Swept Wings in Roll and Sideslip. NACA Rep. 969, 1950.
5. Ribner, Herbert S.: The Stability Derivatives of Low-Aspect-Ratio Triangular Wings at Subsonic and Supersonic Speeds. NACA TN 1423, 1947.
6. Pearson, Henry A., and Jones, Robert T.: Theoretical Stability and Control Characteristics of Wings with Various Amounts of Taper and Twist. NACA Rep. 635, 1938.
7. Zimmerman, Charles H.: An Analysis of Lateral Stability in Power-Off Flight with Charts for Use in Design. NACA Rep. 589, 1937.